*Am J Physiol Regul Integr Comp Physiol* 318: R122–R134, 2020.
First published November 6, 2019; doi:10.1152/ajpregu.00264.2019.

**RESEARCH ARTICLE** | *Obesity, Diabetes and Energy Homeostasis*

# Hypothalamic AMPKα2 regulates liver energy metabolism in rainbow trout through vagal innervation

**Marta Conde-Sieira,[1] Valentina Capelli,[2,3] Rosa Álvarez-Otero,[1] Adrián Díaz-Rúa,[1] Cristina Velasco,[1] Sara Comesaña,[1] Miguel López,[2] and José L. Soengas[1]**

[1]*Laboratorio de Fisioloxía Animal, Departamento de Bioloxía Funcional e Ciencias da Saúde, Facultade de Bioloxía and Centro de Investigación Mariña, Universidade de Vigo, Vigo, Spain;* [2]*Departamento de Fisiología, Grupo NeurObesity, Centro Singular de Investigación en Medicina Molecular y Enfermedades Crónicas, Universidade de Santiago de Compostela-Instituto de Investigación Sanitaria and Centro de Investigación Biomédica en Red-Fisiopatología de la Obesidad y Nutrición, Santiago de Compostela, Spain; and* [3]*Unit of Internal Medicine and Endocrinology, Istituti Clinici Scientifici Maugeri, Department of Internal Medicine and Therapeutics, University of Pavia, Pavia, Italy*

Submitted 3 September 2019; accepted in final form 1 November 2019

**Conde-Sieira M, Capelli V, Álvarez-Otero R, Díaz-Rúa A, Velasco C, Comesaña S, López M, Soengas JL.** Hypothalamic AMPKα2 regulates liver energy metabolism in rainbow trout through vagal innervation. *Am J Physiol Regul Integr Comp Physiol* 318: R122–R134, 2020. First published November 6, 2019; doi:10.1152/ajpregu.00264.2019.—Hypothalamic AMPK plays a major role in the regulation of whole body metabolism and energy balance. Present evidence has demonstrated that this canonical mechanism is evolutionarily conserved. Thus, recent data demonstrated that inhibition of AMPKα2 in fish hypothalamus led to decreased food intake and liver capacity to use and synthesize glucose, lipids, and amino acids. We hypothesize that a signal of abundance of nutrients from the hypothalamus controls hepatic metabolism. The vagus nerve is the most important link between the brain and the liver. We therefore examined in the present study whether surgical transection of the vagus nerve in rainbow trout is sufficient to alter the effect in liver of central inhibition of AMPKα2. Thus, we vagotomized (VGX) or not (Sham) rainbow trout and then intracerebroventricularly administered adenoviral vectors tagged with green fluorescent protein alone or linked to a dominant negative isoform of AMPKα2. The inhibition of AMPKα2 led to reduced food intake in parallel with changes in the mRNA abundance of hypothalamic neuropeptides [neuropeptide Y (*npy*), agouti-related protein 1 (*agrp1*), and cocaine- and amphetamine-related transcript (*cartpt*)] involved in food intake regulation. Central inhibition of AMPKα2 resulted in the liver having decreased capacity to use and synthesize glucose, lipids, and amino acids. Notably, these effects mostly disappeared in VGX fish. These results support the idea that autonomic nervous system actions mediate the actions of hypothalamic AMPKα2 on liver metabolism. Importantly, this evidence indicates that the well-established role of hypothalamic AMPK in energy balance is a canonical evolutionarily preserved mechanism that is also present in the fish lineage.

AMPKα2; food intake; hypothalamus; liver; rainbow trout; vagotomy

## INTRODUCTION

The energy sensor AMP-activated protein kinase (AMPK) is a heterotrimeric protein formed by α (α1 or α2)-, β (β1 or β2)-, and γ (γ1, γ2, or γ3)-subunits (23), and this structure is conserved throughout vertebrate phylogeny (8). In mammals, hypothalamic AMPK is involved in the control of whole body energy homeostasis (25, 28, 30) through regulation of food intake (1, 26, 37), thermogenesis/browning in adipose tissue (5, 27, 33, 35), liver and muscle metabolism (15, 41, 57), or glucose homeostasis (36, 50, 60). Of note, the role of the two different AMPK catalytic α-isoforms is differential. Thus, available studies revealed that in mammals the hypothalamic AMPKα1 isoform is mainly involved in the regulation of peripheral metabolism through thermogenesis in brown adipose tissue and lipid metabolism in liver (27, 33). In contrast, the hypothalamic AMPKα2 isoform is mostly involved in appetite and body weight regulation (2, 24, 51, 55, 57).

In fish, the available knowledge regarding AMPK function mostly refers to peripheral tissues such as liver and muscle (7, 11, 29, 49, 53, 59, 61). In contrast, few studies assessed the role of AMPK in the central nervous system. In rainbow trout (*Oncorhynchus mykiss*) hypothalamus, the phosphorylation status of AMPKα decreased when fish were fed a lipid-enriched diet (22) or nutrient (glucose, oleate, or octanoate) levels rose (42, 56). In a recent study in the same species (4), we observed that food deprivation for 5 days increased the phosphorylation status of AMPKα in the hypothalamus supporting the idea that its well-known role as an energy gauge in mammals was already present in the fish lineage. In the same study, we observed that inhibition of AMPKα1 in the hypothalamus induced slight changes in the hepatic metabolism without modifying food intake. However, inhibition of AMPKα2 in the hypothalamus led to a decrease in food intake and in the ability of the liver to use and synthesize glucose, lipids, and amino acids (4). These results suggested that a signal of abundance of nutrients from the hypothalamus may control liver function, and thus AMPKα2 would play a central role in the regulation of peripheral metabolism in fish, as established in mammals (27, 33). In this regard, the vagus nerve is the most important link between the brain and the liver with both afferent and efferent fibers belonging to the sympathetic and parasympathetic systems. This structure is well conserved throughout evolution, as demonstrated in mammals (6, 33)

Address for reprint requests and other correspondence: J. L. Soengas, Laboratorio de Fisioloxía Animal, Facultade de Bioloxía, Univ. de Vigo, Edificio de Ciencias Experimentais, E-36310 Vigo, Spain (e-mail: jsoengas@uvigo.es).

and fish (39). Therefore, in the present study, we examined whether surgical transection of the vagus nerve is sufficient to alter the effect in liver of central inhibition of AMPKα2.

## MATERIALS AND METHODS

*Fish.* Immature rainbow trout were obtained from a local fish farm (A Estrada, Spain). Fish were maintained for 1 mo in 100-liter tanks under laboratory conditions and a 12:12-h light-dark photoperiod (lights on at 0800, lights off at 2000) in dechlorinated tap water at 15°C. Fish weight at the beginning of the experiment was 108.7 ± 2.8 (SE) g. Fish were fed once daily (1000) to satiety with commercial dry fish pellets (Dibaq-Diproteg SA, Fuentepelayo, Spain; proximate food analysis was 48% crude protein, 14% carbohydrates, 25% crude fat, and 11.5% ash; 20.2 MJ/kg of feed). The experiments described comply with the guidelines of the Council of the European Union (2010/63/UE) and of the Spanish Government (RD 53/2013) for the use of animals in research and were approved by the Ethical Committee for Animal Experimentation of Universidade de Vigo.

*Vagotomy.* Fish were fasted for 24 h before surgery. Individual fish were anesthetized in water containing 2-phenoxyethanol (0.02% vol/vol) and placed on a surgery table covered with wet rubber foam. The gills were continuously irrigated with well-aerated freshwater containing anesthetic. The gastrointestinal tract was denervated through vagotomy (VGX) by cutting the vagi bilaterally following the procedure described by Seth and Axelsson (52). Briefly, the vagus nerve was accessed through a small (0.5 cm) dorsoventral incision in the tissue connecting the fourth gill arch and the cleithrum. Just below the connective tissue the vagus nerves were immediately visible, running parallel to the duct of Cuvier. The vagus was bilaterally sectioned making sure that no part remained intact. This procedure was performed in 24 fish referred to as VGX that were divided into 2 groups of 12 fish each. Sham vagotomy consisted of the same surgical procedure except for transection of the vagus nerve. This was performed in 24 fish, which were also divided into 2 groups of 12 fish each. All sampled fish were checked after being euthanized. Bilateral vagotomy was effective in VGX fish, and vagus nerves were not affected in Sham fish.

*Intracerebroventricular injection of adenoviral vectors.* After VGX or Sham treatments, fish received intracerebroventricular (icv) administration as described previously (45). Briefly, fish ($n$ = 12 fish per group) were placed on a plexiglass board with Velcro straps adjusted to hold them in place. A 29.5-gauge needle attached through a polyethylene cannula to a 10-μL Hamilton syringe was aligned with the sixth preorbital bone at the rear of the eye socket, and from this point, the syringe was moved through the space in the frontal bone into the third ventricle injecting 0.5 μL of adenoviral vectors (ViraQuest, North Liberty, IA) containing green fluorescent protein (GFP) alone (control) or linked to a constitutive inactive isoform of AMPKα2 (AMPKα2-DN; wild type, at 1.1 × 1,012 plaque-forming units/mL). Briefly, aspartate 157 within the α-subunit lies in the conserved DFG motif (subdomain VII in protein kinase catalytic subunits), which has been shown to be essential for MgATP binding in all protein kinases. Mutation of this residue to alanine yields an inactive kinase but does not have any effect on the binding of the β and γ-subunits within the complex. Since formation of the heterotrimeric complex is essential for AMPK activity, overexpression of the inactive α-subunit acts as a dominant negative inhibitor by competing with the native α-subunit for binding with β- and γ-subunits. This approach has been extensively used in mammals (26, 27, 31–33, 35, 51, 58), and we recently demonstrated that the mutation also works properly in fish (4), as expected considering the elevated degree of homology and evolutionary conservation of AMPK (8, 49, 57). The treatment was performed in both Sham and VGX fish. Accordingly, we had four experimental groups ($n$ = 12 fish per group): *1*) Sham fish icv treated with GFP alone, *2*) Sham fish icv treated with GFP linked to AMPKα2-DN, *3*) VGX fish icv treated with GFP alone, and *4*) VGX fish icv treated with GFP linked to AMPKα2-DN. Immediately after injection, fish returned to their experimental tanks.

After 24 h of icv injection, fish were fed, and food intake (FI) was assessed as follows: food was supplied in batches of ~5 g every 2 min until satiation. After feeding, the uneaten food remaining at the bottom (conical tanks) was withdrawn, dried, and weighed. The amount of food consumed by fish was calculated as previously described (47) as the difference from the feed offered. FI values registered after treatment are given with respect to basal values (assessed in each tank throughout the 7 days before icv injection). During the following 18 days after icv injection, fish were supplied with food once a day, and FI levels were recorded as described above.

On the *day 19* after icv treatment, fish (not fed that day) were anesthetized in their holding tanks with 2-phenoxyethanol (0.02% vol/vol) and sampled. Blood was collected by caudal puncture with ammonium-heparinized syringes, and plasma samples were obtained after blood centrifugation, deproteinized immediately (using 0.6 mol/L perchloric acid), and neutralized (using 1 mol/L potassium bicarbonate) before freezing on dry ice and storage at −80°C until further assay. Then, fish were euthanized, and liver samples were taken from all fish in each group for the assessment of enzyme activities, metabolite levels, and mRNA abundance. Whole brains from four fish per group were removed and immediately fixed for histochemical analysis (see below). Brains from the remaining eight fish per group were dissected, and the hypothalamus was snap-frozen and stored at −80°C to be used later for assessment by Western blot of changes in the levels of acetyl-CoA carboxylase-α (Accα) and phospho-Accα (pAccα), mRNA abundance of neuropeptides by quantitative real-time PCR (RT-qPCR), and enzyme activities and metabolite levels by spectrophotometry.

*Immunohistochemical analyses.* Sampled brains ($n$ = 4 brains per group) were immediately fixed by immersion in 4% paraformaldehyde in 0.1 M phosphate-buffered saline (PBS) at pH 7.4 for 24 h at 4°C. Pieces were then dehydrated in a graded series of alcohols and embedded in paraffin. Serial transverse sections ranging from 7 to 10 μm were obtained and processed for immunohistochemistry. Alternate sections were stained using hematoxylin-eosin to study the overall structure. The primary antibody used in this study was polyclonal rabbit anti-GFP (ab-290; Abcam), whose specificity was previously tested by Western blot analysis (4). Sections were processed as follows: *1*) preincubation with 0.1% bovine serum albumin (BSA) in PBS containing 0.25% Triton X-100 (PBS-T) for 1 h, to inhibit nonspecific reactivity; *2*) incubation with anti-GFP (1:100; Abcam) antibody diluted 1:100 in PBS-T overnight at room temperature in a humid chamber; and *3*) incubation with secondary specific antibody (Alexa Fluor 488 goat anti-rabbit conjugated; Invitrogen) diluted 1:400 in PBS-T. After incubation, sections were washed in PBS-T and coverslipped using ProLong Gold with DAPI (Molecular Probes) to delay fluorescence fading. Immunostaining was not observed when primary antisera were omitted from the protocol. In addition, an untreated trout was processed in parallel to confirm the specificity of immunostaining, and no immunoreactivity was observed (results not shown). Slides were observed and photographed using an Olympus microscope (BX51) equipped with a digital camera (Olympus DP71). The images were composed and labeled with CorelDRAW Software (Corel Corporation).

*Assessment of metabolite levels and enzyme activities.* Plasma glucose, lactate, triglyceride, and fatty acid levels were determined enzymatically using commercial kits [Spinreact (Barcelona, Spain) for glucose, lactate, and triglyceride levels and Wako Chemicals (Neuss, Germany) for fatty acid levels] adapted to a microplate format. Total α-amino acid levels were assessed using the nynhydrin method (38), with alanine as standard.

Samples used to assess metabolite levels in liver were homogenized immediately with the ultrasonic disrupter UP200H (Hielscher, Teltow, Germany) with 5 bursts at 24 kHz, 50% amplitude, and 0.5 cycles in 7.5 volumes of ice-cooled 0.6 mol/L perchloric acid and

neutralized (using 1 mol/L potassium bicarbonate). The homogenate was centrifuged (10,000 *g*), and the supernatant was used to assay tissue metabolites. Glycogen levels were assessed using the method of Keppler and Decker (16). Levels of glucose obtained after glycogen breakdown (after subtracting free glucose levels) and lactate, triglyceride, and fatty acid levels were determined colorimetrically, as described above for plasma samples.

Samples used to assess metabolite levels in liver were homogenized immediately with the ultrasonic disrupter UP200H as described above with 9 volumes of ice-cold stopping buffer containing 50 mmol/L imidazole-HCl (pH 7.6), 15 mmol/L 2-mercaptoethanol, 100 mmol/L potassium fluoride, 5 mmol/L EDTA, 5 mmol/L EGTA, and a protease inhibitor cocktail (Sigma Chemical Co., St. Louis, MO). The homogenate was centrifuged, and the supernatant was used immediately for enzyme assays. Enzyme activities were determined using microplate reader INFINITE 200 Pro (Tecan, Männedorf, Switzerland). Reaction rates of enzymes were determined by the decrease in absorbance of NADH at 340 nm. The reactions were started by the addition of supernatant (15 μL) at a preestablished protein concentration, omitting the substrate in control wells (final volume 265–295 μL) and allowing the reactions to proceed at 20°C for preestablished time periods (10–45 min). Enzyme activities are expressed per protein level, which was assayed with the bicinchoninic acid method with BSA (Sigma) as standard. Enzyme activities were assessed at maximum rates determined by preliminary tests to determine optimal substrate concentrations. Glucokinase [Gck, Enzyme Commission no. (EC) 2.7.1.2], glycogen synthase (Gsase, EC 1.1.1.35), glycogen phosphorylase (Gpase, EC 2.4.1.1), fructose 1,6-bisphosphatase (Fbpase, EC 3.1.3.11.), carnitine palmitoyl transferase 1a (Cpt-1, *EC* 2.3.1.21), fatty acid synthase (Fas, EC 2.3.1.85), glutamate dehydrogenase (Gdh, EC 1.4.1.4), and glutamate-pyruvate transaminase (Gpt, EC 2.6.1.15) activities were determined as described previously (21, 46, 48).

*Western blot analysis.* Total protein of samples was extracted using TRIzol reagent (Life Technologies, Grand Island, NY) following the manufacturer's protocol for protein isolation. The protein pellet obtained was solubilized in 100 μL of buffer containing 150 mmol/L NaCl, 10 mmol/L Tris·HCl, 1 mmol/L EGTA, 1 mmol/L EDTA (pH 7.4), 100 mmol/L sodium fluoride, 4 mmol/L sodium pyrophosphate, 2 mmol/L sodium orthovanadate, 1% Triton X-100, 0.5% Nonidet P-40-Igepal, and 1.02 mg/mL protease inhibitor cocktail (Sigma). Tubes were kept on ice during the whole process to prevent protein denaturation and stored at −80°C at the end of the process. The concentration of protein in each sample was determined using Bradford assay with BSA as standard. Hypothalamic protein lysates (10 μg) were subjected to SDS-PAGE, electrotransferred to polyvinylidene difluoride membranes (Millipore, Billerica, MA) with a semidry blotter, and probed with anti-pAccα and anti-Accα antibodies (Cell Signaling Technology, Leiden, The Netherlands; 1:1,000 dilution) as previously described (26, 27, 31–33, 35, 51, 58). Each membrane was then incubated with the corresponding anti-rabbit IgG-horseradish peroxidase secondary antibody (Dako, Glostrup, Denmark). The membranes were exposed to an X-ray film (Fujifilm, Tokyo, Japan) and developed using developer G150 (AGFA HealthCare, Mortsel, Belgium) and Fixator G354 (AGFA HealthCare). Autoradiographic films were scanned, and the band signal was quantified by densitometry using ImageJ-1.33 software (National Institutes of Health, Bethesda, MD). Anti-pAccα and anti-Accα antibodies cross-react successfully with proteins of interest in rainbow trout hypothalamus (4). Antibodies were previously validated by comparing blots obtained after loading different quantities of protein from rainbow trout hypothalamus with those obtained in the same tissue in rat.

*mRNA abundance analysis by RT-qPCR.* Total RNA was extracted using TRIzol reagent (Life Technologies) and subsequently treated with RQ1-DNase (Promega, Madison, WI) according to the manufacturer's instructions. RNA quantity was assessed with a NanoVue Plus spectrophotometer (GE Healthcare Life Sciences, Pittsburgh, PA) with ratio of absorbance at 260 and 280 nm. RNA integrity was determined by gel electrophoresis (28S and 18S bands). Two micrograms of total RNA were reverse transcribed using SuperScript II reverse transcriptase (Promega), RNase inhibitor, and random hexamers (Promega) to obtain 20 μL.

Gene expression levels were determined by RT-qPCR using the iCycler iQ (Bio-Rad, Hercules, CA). Analyses were performed per duplicate with 1 μL cDNA and 500 nM of each forward and reverse primer, in 15-μL reaction volume of Maxima SYBR Green qPCR Master Mix (Life Technologies) containing Maxima Hot Start Taq DNA Polymerase, 2-deoxynucleotide 5′-triphosphates, 2-deoxyuridine 5′-triphosphates, and SYBR Green in PCR buffer. Sequences of the forward and reverse primers used for each gene expression are shown in Table 1. Relative quantification of the target gene transcript was done using *actb* (encoding β-actin) and *eef1a1* (encoding elongation factor 1α) gene expressions as reference, which were stably expressed in this experiment. Thermal cycling was initiated with incubation at 95°C for 90 s using hot-start iTaq DNA polymerase

Table 1. *Nucleotide sequences of the PCR primers used to evaluate mRNA abundance by RT-qPCR*

| | Forward Primer | Reverse Primer | Annealing Temperature, °C | Database | Accession No. | Size, bp | Efficiency, % | $R^2$ |
|---|---|---|---|---|---|---|---|---|
| *actb* | GATGGGCCAGAAAGACAGCTA | TCGTCCCAGTTGGTGACGAT | 59 | GenBank | NM_001124235.1 | 105 | 90.1 | 0.997 |
| *agrp1* | ACCAGCAGTCCTGTCTGGGTAA | AGTAGCAGATGGAGCCGAACA | 60 | GenBank | CR376289 | 87 | 90.7 | 0.986 |
| *cartpt* | ACCATGGAGAGCTCCAG | GCGCACTGCTCTCCAA | 60 | GenBank | NM_001124627 | 275 | 91.5 | 0.932 |
| *cpt1a* | TCGATTTTCAAGGGTCTTCG | CACAACGATCAGCAAACTGG | 55 | GenBank | AF327058 | 166 | 93.5 | 0.928 |
| *eef1a1* | TCCTCTTGGTCGTTTCGCTG | ACCCGAGGGACATCCTGTG | 59 | GenBank | AF498320 | 159 | 99.4 | 0.987 |
| *fasn* | GAGACCTAGTGGAGGCTGTC | TCTTGTTGATGGTGAGCTGT | 59 | SIGENAE | tcab0001c.e.065.1.s.om.8 | 161 | 95.7 | 0.995 |
| *fbp1* | GCTGGACCCTTCCATCGG | CGACATAACGCCCACCATAGG | 59 | GenBank | AF333188 | 182 | 94.3 | 0.990 |
| *glud1* | TGCTGACACCTATGCCAACAC | CCTGGCTGATGGGCTTACC | 58 | GenBank | AJ556997 | 80 | 93.3 | 0.973 |
| *gck* | GCACGGCTGAGATGCTCTTTG | GCCTTGAACCCTTTGGTCCAG | 60 | GenBank | AF053331 | 250 | 95.6 | 0.998 |
| *gpt* | CTGGGCTGTTCGTCACTTCA | AATGACTGCGACAGGACAATGT | 58 | GenBank | BT045760 | 57 | 95.6 | 0.975 |
| *gys1* | CGTGGTGAGAGGAAGGAACTGAGC | CCGTTGAGACCGTGGAGACA | 59 | GenBank | BT073381.1 | 236 | 99.5 | 0.981 |
| *npy* | CTCGTCTGGACCTTTATATGC | GTTCATCATATCTGGACTGTG | 58 | GenBank | NM_001124266 | 247 | 99.0 | 0.912 |
| *pfk* | GGTGGAGATGCACAAGGAAT | CTTGATGTTGTCCCCTCCAT | 59 | SIGENAE | tcbk0069c.k.05_s.1 | 158 | 89.9 | 0.957 |
| *pomca1* | CTCGCTGTCAAGACCTCAACTCT | GAGTTGGGTTGGAGATGGACCTC | 60 | TIGR | TC86162 | 95 | 90.0 | 0.991 |
| *pygl* | GCCCATCCCTGGATATATGA | GACCACAGCCTCATGGTGTT | 60 | GenBank | XM_021574890.1 | 101 | 90.8 | 0.984 |

RT-qPCR, quantitative real-time PCR; SIGENAE, Système d'information pour l'analyse des génomes des animaux d'élevage; TIGR, The Institute for Genomic Research. Genes: *actb*, β-actin; *agrp1*, agouti-related protein 1; *cartpt*, cocaine- and amphetamine-related transcript; *cpt1a*, carnitine palmitoyl transferase 1a; *eef1a1*, elongation factor 1α; *fasn*, fatty acid synthase; *fbp1*, fructose 1,6-bisphosphatase; *gck*, glucokinase; *glud1*, glutamate dehydrogenase; *gpt*, glutamate-pyruvate transaminase; *gys1*, glycogen synthase; *npy*, neuropeptide Y; *pfk*, 6-phosphofructo-1-kinase; *pomca1*, pro-opiomelanocortin a1; *pygl*, glycogen phosphorylase.

activation followed by 35 cycles, each one consisting of heating at 95°C for 20 s and specific annealing and extension temperatures for 20 s. Calibration curves were made with serial dilutions of cDNA (by triplicate). Only efficiency values between 90 and 100% were accepted (the $R^2$ for all the genes assessed was always higher than 0.985). The specificity of amplifications was checked by melting curves, which were systematically monitored (55°C temperature gradient at 0.5°C/s from 55 to 94°C) to ensure that only one fragment was amplified. The PCR products were checked by electrophoresis on a 1.5% agarose gel. The corresponding bands were cut from the gel, purified with the QIAquick Gel Extraction Kit (Qiagen, Hilden, Germany), and sequenced in an Applied Biosystems 3130 genetic analyzer (Foster City, CA) in Servicio de Determinación Estructural, Proteómica y Genómica (Centro de Apoio Científico e Tecnolóxico á Investigación, Universidade de Vigo). The obtained sequences satisfactorily matched the reference database sequences after comparing

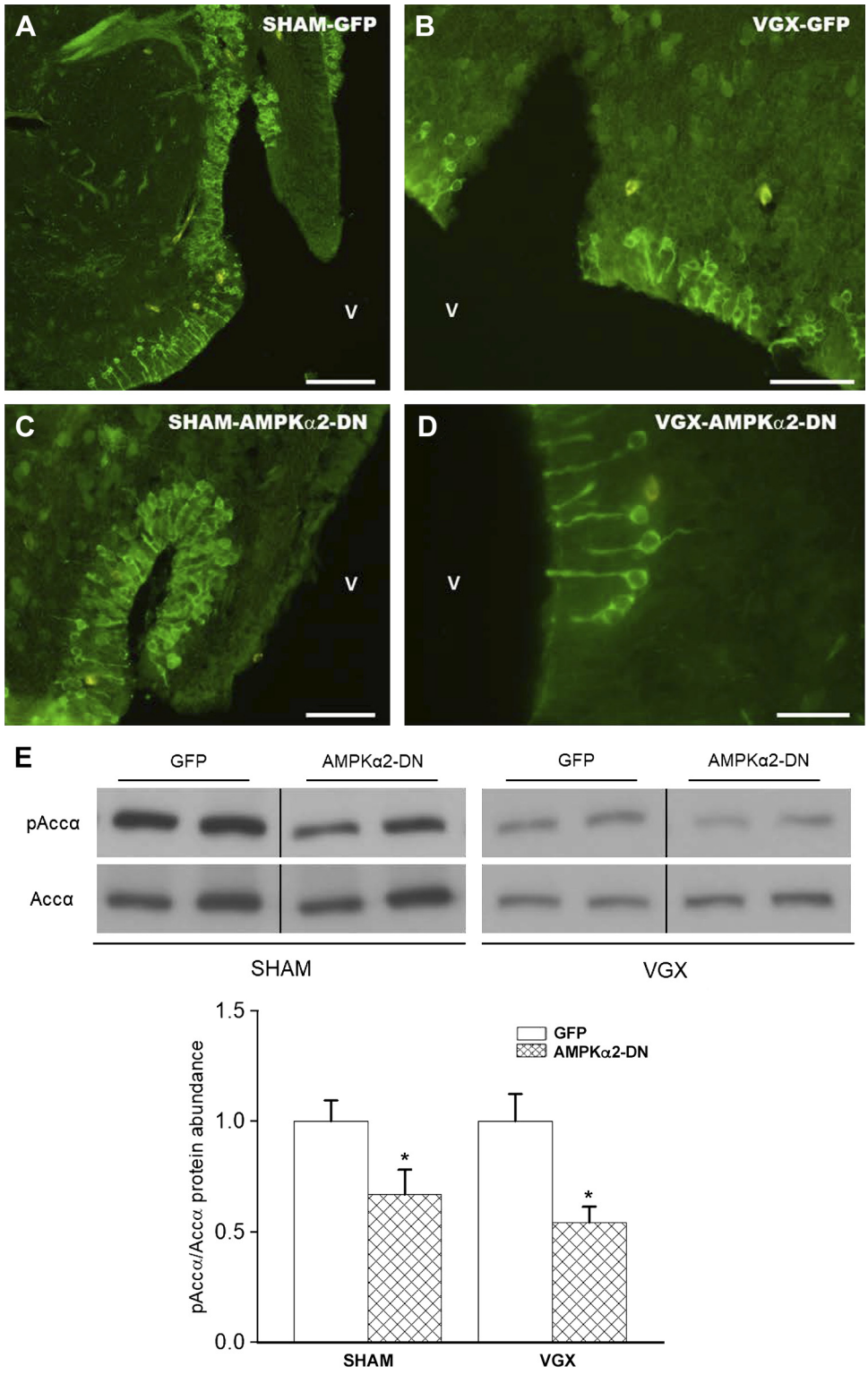


Fig. 1. Photomicrographs of transverse sections through the third ventricle (V) of rainbow trout brain showing green fluorescent protein immunoreactivity (GFP-ir) 19 days after intracerebroventricular administration of adenovirus tagged with GFP (*A* and *B*) or dominant negative isoform of AMPKα2 (AMPKα2-DN; *C* and *D*) in Sham (*A* and *C*) or vagotomized (VGX; *B* and *D*) fish. The image in *D* shows a detail of bipolar morphology with a long and thin process that ended in the ventricle. Scale bars: 100 μm (*A*), 50 μm (*B* and *C*), and 25 μm (*D*). Protein levels of phospho-acetyl-CoA carboxylase-α (pAccα) relative to Accα (*E*) in the hypothalamus of rainbow trout 19 days after intracerebroventricular administration of adenovirus tagged with GFP or AMPKα2-DN in Sham or VGX fish. Ten micrograms of total protein were loaded on the gel per lane. Western blots were performed on 6 individual samples per treatment, and 2 representative blots are shown. Graphs represent the ratio between pAccα and total Accα. Each value is the mean ± SE of $n = 6$ fish per group. *Significantly different ($P < 0.05$) from GFP within Sham or VGX.

them with the Basic Local Alignment Search Tool (BLAST) program. Samples without reverse transcriptase and samples without RNA were run for each reaction as negative controls. Relative quantification of the target gene transcript with the *actb* and *eef1a1* reference gene transcripts was made following the Pfaffl method (44).

*Statistical analysis.* Comparisons among groups were performed using two-way ANOVA with surgery (Sham and VGX) and treatment (GFP and AMPKα2-DN) as main factors. The normal distribution of variables and homoscedasticity were analyzed by Kolmogorov–Smirnov tests. Post hoc comparisons were performed by a Šidák test. Comparisons were performed with the SigmaStat statistical package, and differences were considered statistically significant at $P < 0.05$.

## RESULTS

*Central administration of adenoviral vectors expressing AMPKα2-DN promoted an anorectic effect.* To elucidate the contribution of hypothalamic AMPKα2 activity to energy balance, adenoviruses encoding a dominant negative isoform of AMPKα2 (AMPKα2-DN) or control adenovirus expressing GFP alone (5, 27, 31–33, 35, 51, 58) were icv injected into rainbow trout. Infection efficiency was assessed by hypothalamic expression of GFP in all the groups (Fig. 1, *A–D*), as well as decreased phosphorylation of acetyl-CoA carboxylase (pAcc) in the hypothalamus (Fig. 1*E*).

The administration of adenoviral vectors expressing GFP alone or linked to AMPKα2-DN was appropriate, as judged by photomicrographs of hypothalamic sections showing GFP immunoreactivity (GFP-ir) in all groups assessed. GFP-ir was observed in the hypothalamic third ventricle in cells that present morphological features in common with cerebrospinal fluid-contacting cells, as commented in a previous study using the same methodology (4). Increased phosphorylation of ACCα is a typical downstream response of AMPKα2 activation (1, 37), and therefore we expected a decrease under conditions of AMPKα2 inhibition considering the high similarity of ACC between mammals and fish (8). The decrease observed in pAccα levels after AMPKα2-DN treatment either in Sham or VGX fish (Fig. 1*E*) clearly supports hypothalamic inhibition of AMPKα2. These results are also comparable to those observed in a prior study (4), thus validating the experimental design.

The values of food intake (Fig. 2) are presented as daily values of the percentage of weight of eaten food with respect to the basal levels of each group ($n = 12$ fish). The average was calculated from *day 7* (time needed for food intake to stabilize) until *day 18* after icv treatment. A lower FI was observed in the AMPKα2-DN group with respect to GFP in Sham, but it did not reach statistical significance ($P = 0.089$) in the VGX group. As occurs in mammals, food intake in the VGX groups was lower than that in Sham groups, for both GFP and AMPKα2-DN treatments.

*Central administration of adenoviral vectors expressing AMPKα2-DN modulated neuropeptide expression in the hypothalamus.* In keeping with the observed anorectic effects, the mRNA abundance of neuropeptide Y (*npy*) decreased after AMPKα2-DN treatment compared with GFP both in Sham and VGX groups (Fig. 3*A*). Similarly, the mRNA abundance of agouti-related protein 1 (*agrp1*) decreased after AMPKα2-DN treatment compared with GFP in the Sham group but not with AMPKα2-DN treatment in the VGX group (Fig. 3*B*). Cocaine- and amphetamine-related transcript (*cartpt*) mRNA abundance increased after AMPKα2-DN treatment compared with GFP in the Sham group (Fig. 3*C*). Finally, no significant changes occurred for pro-opiomelanocortin a1 (*pomca1*) mRNA abundance in any of the experimental settings (Fig. 3*D*).

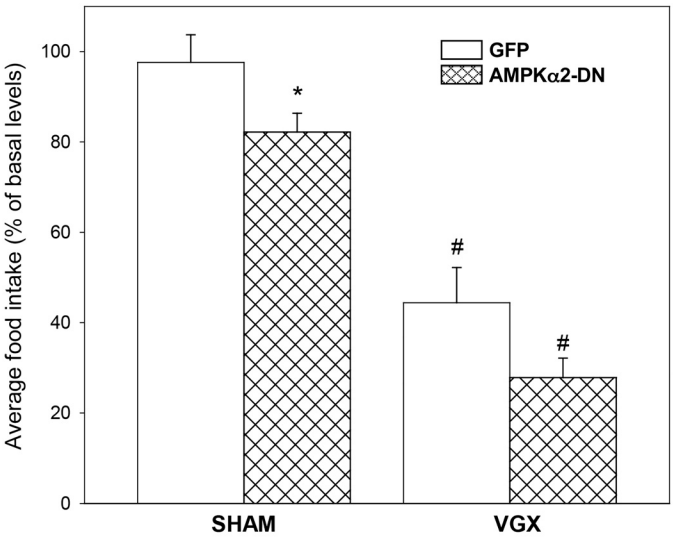


Fig. 2. Average daily food intake registered in rainbow trout from *day 7* to *day 18* after intracerebroventricular administration of adenovirus tagged with green fluorescent protein (GFP) or dominant negative isoform of AMPKα2 (AMPKα2-DN) in Sham or vagotomized (VGX) fish. Food intake is displayed as the percentage of food ingested with respect to baseline levels (calculated as the average of food intake on the 7 days previous to experiment). Each value is the mean ± SE of $n = 12$ fish per treatment. *Significantly different ($P < 0.05$) from GFP within Sham or VGX; #significantly different ($P < 0.05$) from Sham within GFP or AMPKα2-DN.

*Central administration of adenoviral vectors expressing AMPKα2-DN regulated plasma metabolites.* Levels of glucose in plasma decreased after AMPKα2-DN treatment compared with GFP in both Sham and VGX groups (Fig. 4*A*). Lactate levels in plasma decreased after AMPKα2-DN treatment compared with GFP in the Sham group (Fig. 4*B*). Levels of fatty acid increased after AMPKα2-DN treatment compared with GFP in the Sham group, whereas levels after GFP treatment were higher in the VGX group than in the Sham group (Fig. 4*C*). The levels of triglyceride in plasma (Fig. 4*D*) decreased after AMPKα2-DN treatment compared with GFP in the Sham group, whereas levels after GFP treatment were lower in the VGX group than in the Sham group. Finally, amino acid levels in plasma (Fig. 4*E*) increased after treatment with AMPKα2-DN compared with GFP in the Sham group and compared with the same treatment in the VGX group. Overall, this evidence indicated that hypothalamic inhibition of AMPKα2 function impacted circulating levels of metabolites and that VGX did not impair that effect.

*Central administration of adenoviral vectors expressing AMPKα2-DN modulated hepatic metabolism.* Metabolite levels in liver are shown in Fig. 5. No significant changes occurred in the levels of glucose (Fig. 5*A*) and triglycerides (Fig. 5*D*). The levels of glycogen (Fig. 5*B*) and lactate (Fig. 5*C*) were lower in the VGX group than in the Sham group. The levels of fatty acid (Fig. 5*E*) decreased after AMPKα2-DN treatment compared with GFP in the Sham group, whereas levels after GFP treatment were lower in the VGX group than in the Sham group. Finally, amino acid levels (Fig. 5*F*) increased after AMPKα2-DN treatment compared with GFP in the Sham

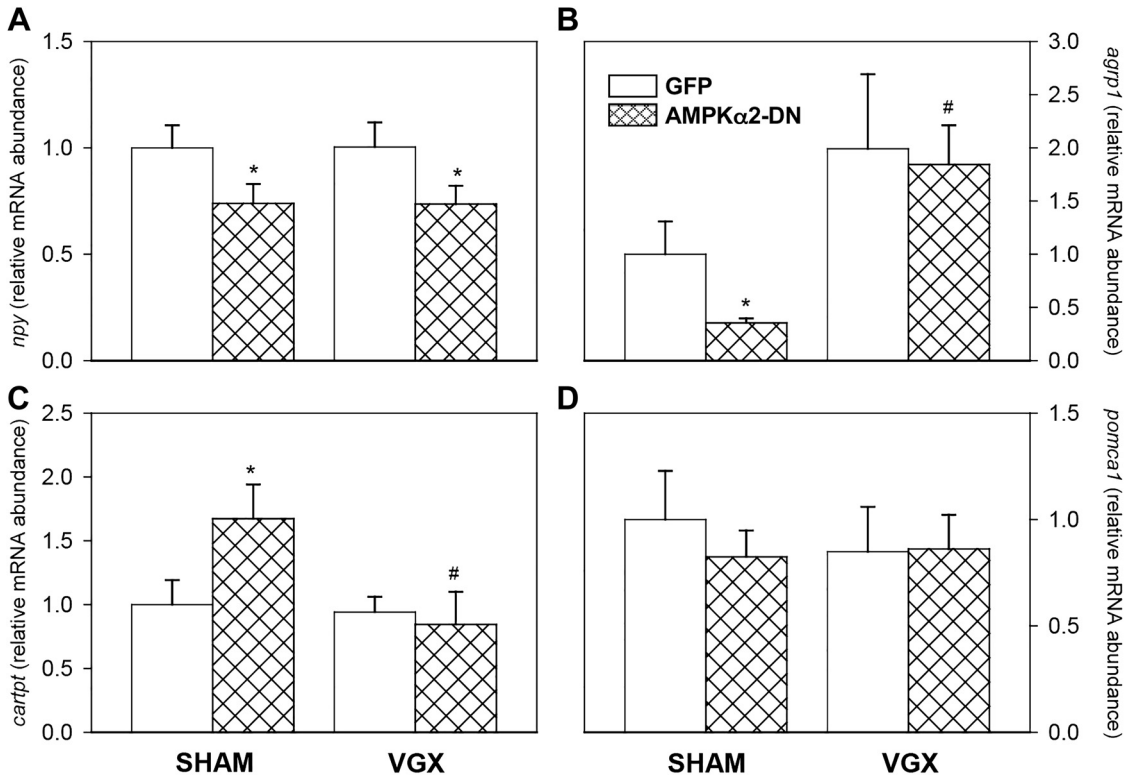


Fig. 3. mRNA abundance of neuropeptide Y (*npy*, *A*), agouti-related protein 1 (*agrp1*, *B*), cocaine- and amphetamine-related transcript (*cartpt*, *C*), and pro-opiomelanocortin a1 (*pomca1*, *D*) in the hypothalamus of rainbow trout 19 days after intracerebroventricular administration of adenovirus tagged with green fluorescent protein (GFP) or dominant negative isoform of AMPKα2 (AMPKα2-DN) in Sham or vagotomized (VGX) fish. Gene expression results are standardized to the Sham-GFP group and are normalized by β-actin (*actb*) and elongation factor 1α (*eef1a1*) expression. Each value is the mean ± SE of $n = 6$ fish per group. *Significantly different ($P < 0.05$) from GFP within Sham or VGX; #significantly different ($P < 0.05$) from Sham within GFP or AMPKα2-DN.

group and compared with the same treatment in the VGX group.

Next, we examined the activity and mRNA abundance of enzymes involved in glucose metabolism, shown in Fig. 6. The activity of Gck decreased in VGX groups compared with Sham groups both after GFP and after AMPKα2-DN treatments (Fig. 6*A*). The mRNA abundance of *gck* (Fig. 6*B*) decreased after AMPKα2-DN treatment compared with GFP in Sham fish, whereas values in VGX groups were lower than those of Sham fish both after GFP and after AMPKα2-DN treatment. 6-Phosphofructo-1-kinase (Pfk) activity (Fig. 6*C*) decreased after AMPKα2-DN treatment compared with GFP in Sham fish and compared with AMPKα2-DN treatment in VGX fish. Gsase activity after AMPKα2-DN treatment was lower in VGX than in Sham fish (Fig. 6*E*). Gpase activity after AMPKα2-DN treatment was higher in VGX than in Sham fish (Fig. 6*G*). Fbpase activity (Fig. 6*I*) decreased after AMPKα2-DN treatment compared with GFP in Sham fish, whereas values in VGX groups were higher than those of Sham fish both after GFP and after AMPKα2-DN treatment. Finally, no significant changes occurred in mRNA abundance of *pfk* (Fig. 6*D*), glycogen synthase (*gys1*, Fig. 6*F*), glycogen phosphorylase (*pygl*, Fig. 6*H*), or fructose 1,6-bisphosphatase (*fbp1*, Fig. 6*J*).

The activity and mRNA abundance of enzymes involved in lipid and amino acid metabolism are shown in Fig. 7. As expected, Cpt-1 activity (Fig. 7*A*) decreased after AMPKα2-DN treatment compared with GFP in Sham fish and compared with AMPKα2-DN treatment in VGX fish. The mRNA abundance of carnitine palmitoyl transferase 1a (*cpt1a*) was higher in the VGX group than in the Sham group both after GFP and after AMPKα2-DN treatment (Fig. 7*B*). Fas activity was lower in VGX than in Sham fish after GFP treatment (Fig. 7*C*). The mRNA abundance of fatty acid synthase (*fasn*, Fig. 7*D*) decreased after AMPKα2-DN treatment compared with GFP in VGX fish, whereas values in VGX fish were lower than those of Sham fish both after GFP and after AMPKα2-DN treatment. The mRNA abundance of glutamate dehydrogenase (*glud1*, Fig. 7*F*) decreased after AMPKα2-DN treatment compared with GFP in Sham fish, whereas values after GFP treatment were lower in VGX than in Sham fish. Finally, no significant changes were observed in the activities of Gdh (Fig. 7*E*) or Gpt (Fig. 7*G*) or mRNA abundance of *gpt* (Fig. 7*H*).

## DISCUSSION

Our data show that the treatment with AMPKα2-DN induced a decrease in food intake of Sham fish, which is comparable to that observed previously in control fish of the same species after a similar icv treatment (4). This result reinforces the role of AMPKα2 in the modulation of food intake in fish. To further support such a role, we have evaluated changes in mRNA abundance of *npy*, *agrp*, *pomc*, and *cartpt* showing changes in mammalian hypothalamus after AMPKα activation (25, 30). In Sham fish we observed a clear decrease

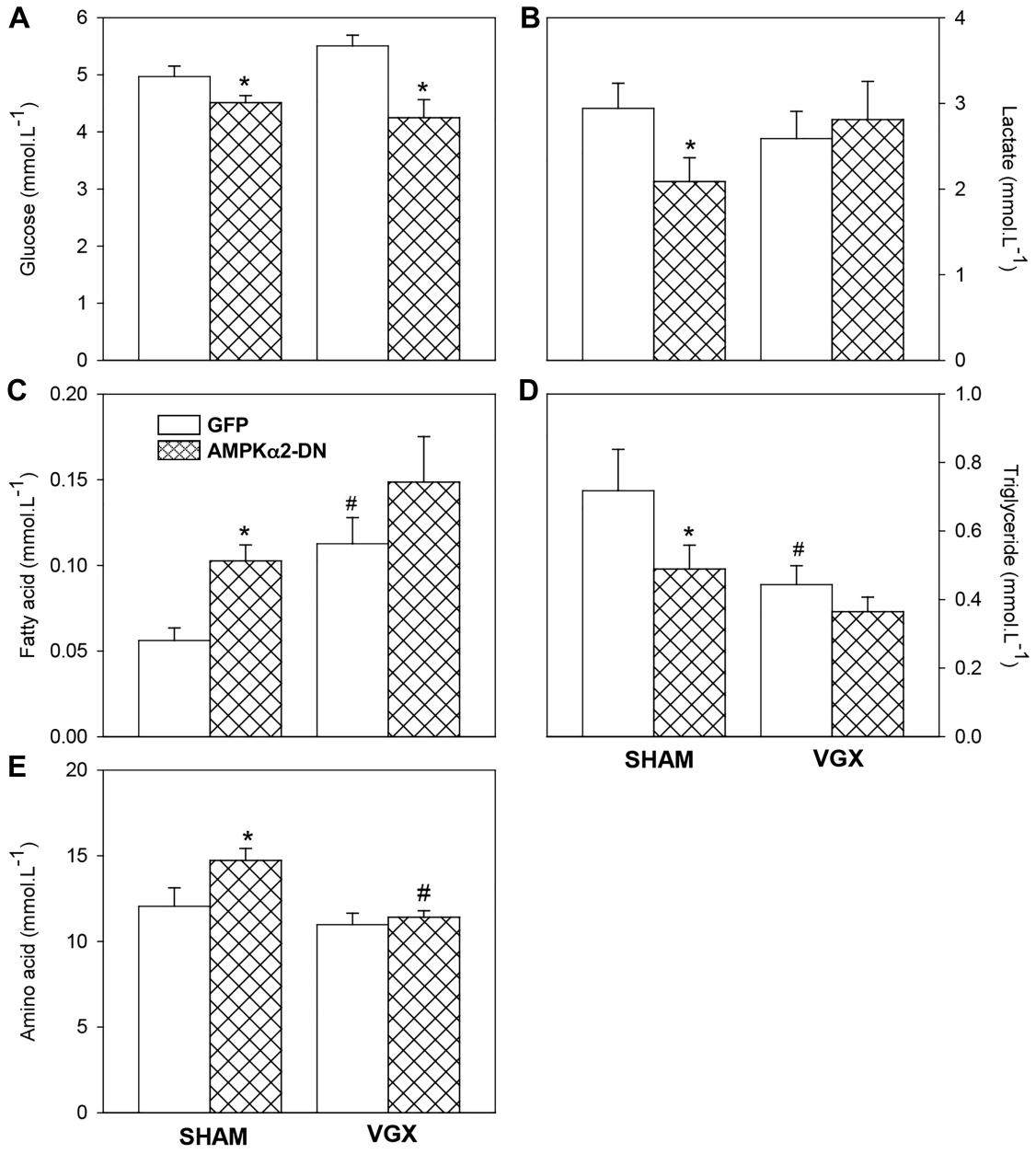


Fig. 4. Levels of glucose (*A*), lactate (*B*), fatty acids (*C*), triglycerides (*D*), and amino acids (*E*) in plasma of rainbow trout 19 days after intracerebroventricular administration of adenovirus tagged with green fluorescent protein (GFP) or dominant negative isoform of AMPKα2 (AMPKα2-DN) in Sham or vagotomized (VGX) fish. Each value is the mean ± SE of $n = 12$ fish per treatment. *Significantly different ($P < 0.05$) from GFP within Sham or VGX; #significantly different ($P < 0.05$) from Sham within GFP or AMPKα2-DN.

in the mRNA abundance of the orexigenic *npy* and *agrp1*, which is in agreement with the decreased mRNA abundance of the same neuropeptides observed in mice after a comparable adenoviral treatment (37). We also observed an increase in the mRNA abundance of the anorexigenic *cartpt*, whereas no changes occurred in levels of *pomca1*. With the exception of the lack of changes in *pomca1*, changes observed clearly indicate that under conditions of AMPKα2 inhibition a decrease in the orexigenic potential occurred in the hypothalamus. This is the first time in which changes in neuropeptide mRNA abundance were observed in fish hypothalamus after AMPK inhibition, which fits with the decreased feeding observed in the same group. Changes in neuropeptides are also in agreement with those previously observed in the hypothalamus of the same species under anorectic conditions resulting from hormone treatments or raised levels of nutrients [reviewed by Conde-Sieira and Soengas (3), Delgado et al. (9), and Soengas et al. (54)].

The treatment with AMPKα2-DN in Sham fish also affected metabolic parameters in plasma and liver indicative of the peripheral effects of central AMPKα2. These results are in general comparable to those observed before (4), thus supporting the experimental design, though in some cases no significant changes, only trends, occurred. Thus, in plasma, changes observed in Sham fish comparable to those observed before included levels of glucose, fatty acids, triglycerides, and amino

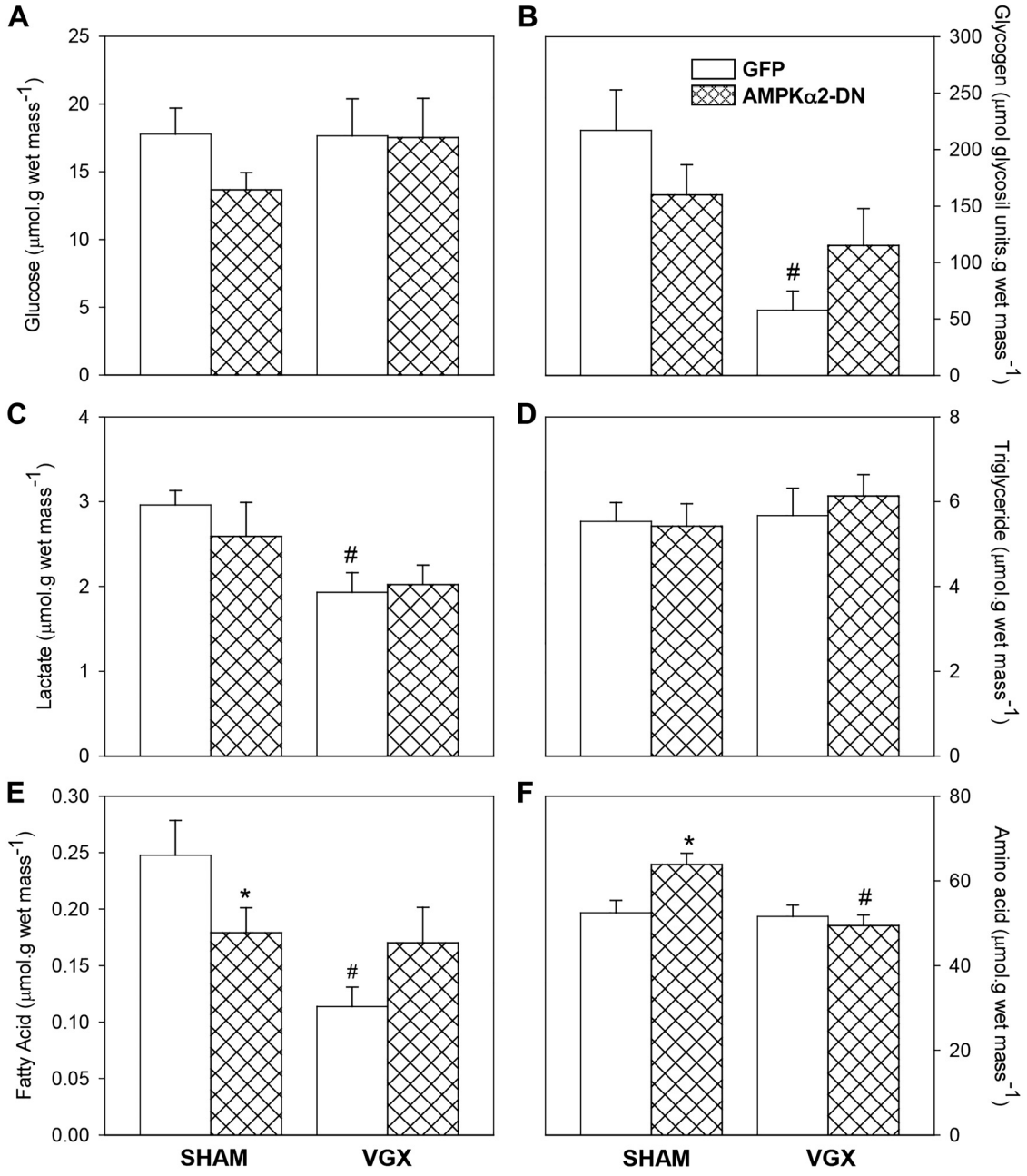


Fig. 5. Levels of glucose (*A*), glycogen (*B*), lactate (*C*), triglycerides (*D*), fatty acids (*E*), and amino acids (*F*) in liver of rainbow trout 19 days after intracerebroventricular administration of adenovirus tagged with green fluorescent protein (GFP) or dominant negative isoform of AMPKα2 (AMPKα2-DN) in Sham or vagotomized (VGX) fish. Each value is the mean ± SE of $n = 12$ fish per treatment. *Significantly different ($P < 0.05$) from GFP within Sham or VGX; #significantly different ($P < 0.05$) from Sham within GFP or AMPKα2-DN.

acids (not significant). In liver, comparable responses were also detected in the levels of fatty acids and amino acids, the activities of Pfk, Fbpase, and Cpt-1, and mRNA abundance of *gck* and *glud1*, whereas similar trends (not significant) occurred for levels of glucose, glycogen, and lactate, the activities of Fas and Gpt, and mRNA abundance of *gpt*. Therefore, central AMPKα2 affects liver energy metabolism, and this subsequently affects levels of metabolites in plasma. In gen-

Fig. 6. Enzyme activity (*A*, *C*, *E*, *G*, and *I*) and mRNA abundance (*B*, *D*, *F*, *H*, and *J*) of glucokinase [Gck (*gck*)], 6-phosphofructo-1-kinase [Pfk (*pfk*)], glycogen synthase [Gsase (*gys1*)], glycogen phosphorylase [Gpase (*pygl*)], and fructose 1,6-bisphosphatase [Fbpase (*fbp1*)] in liver of rainbow trout 19 days after intracerebroventricular administration of adenovirus tagged with green fluorescent protein (GFP) or dominant negative isoform of AMPKα2 (AMPKα2-DN) in Sham or vagotomized (VGX) fish. Gene expression results are standardized to the Sham-GFP group and are normalized by β-actin (*actb*) and elongation factor 1α (*eef1a1*) expression. Each value is the mean ± SE of $n = 12$ (enzyme activities) or $n = 6$ (mRNA abundance) fish per group. *Significantly different ($P < 0.05$) from GFP within Sham or VGX; #significantly different ($P < 0.05$) from Sham within GFP or AMPKα2-DN.

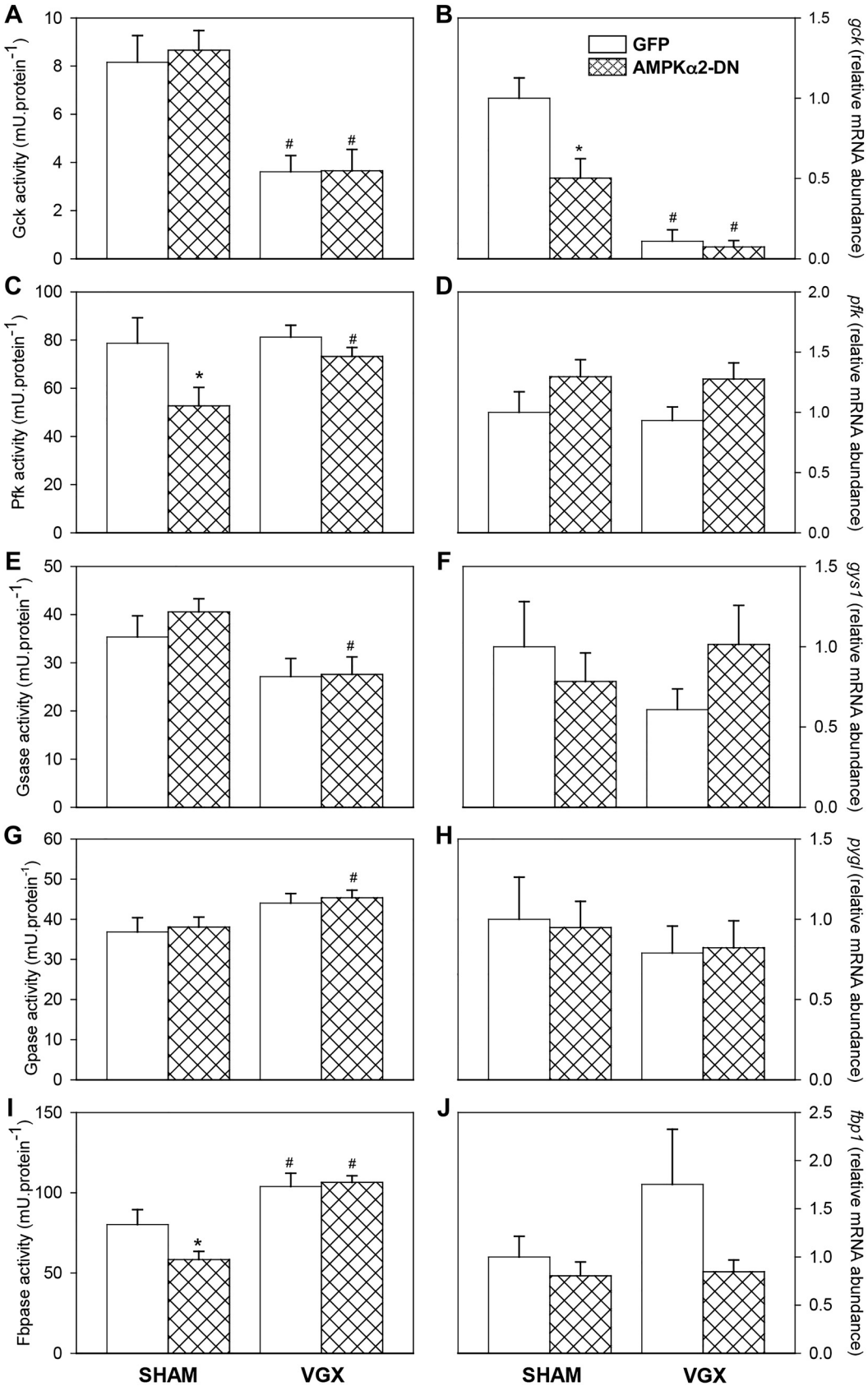
A
Gck activity (mU.protein-1)
B
GFP
AMPKα2-DN
gck (relative mRNA abundance)
C
Pfk activity (mU.protein-1)
D
pfk (relative mRNA abundance)
E
Gsase activity (mU.protein-1)
F
gys1 (relative mRNA abundance)
G
Gpase activity (mU.protein-1)
H
pygl (relative mRNA abundance)
I
Fbpase activity (mU.protein-1)
J
fbp1 (relative mRNA abundance)
SHAM
VGX
SHAM
VGX

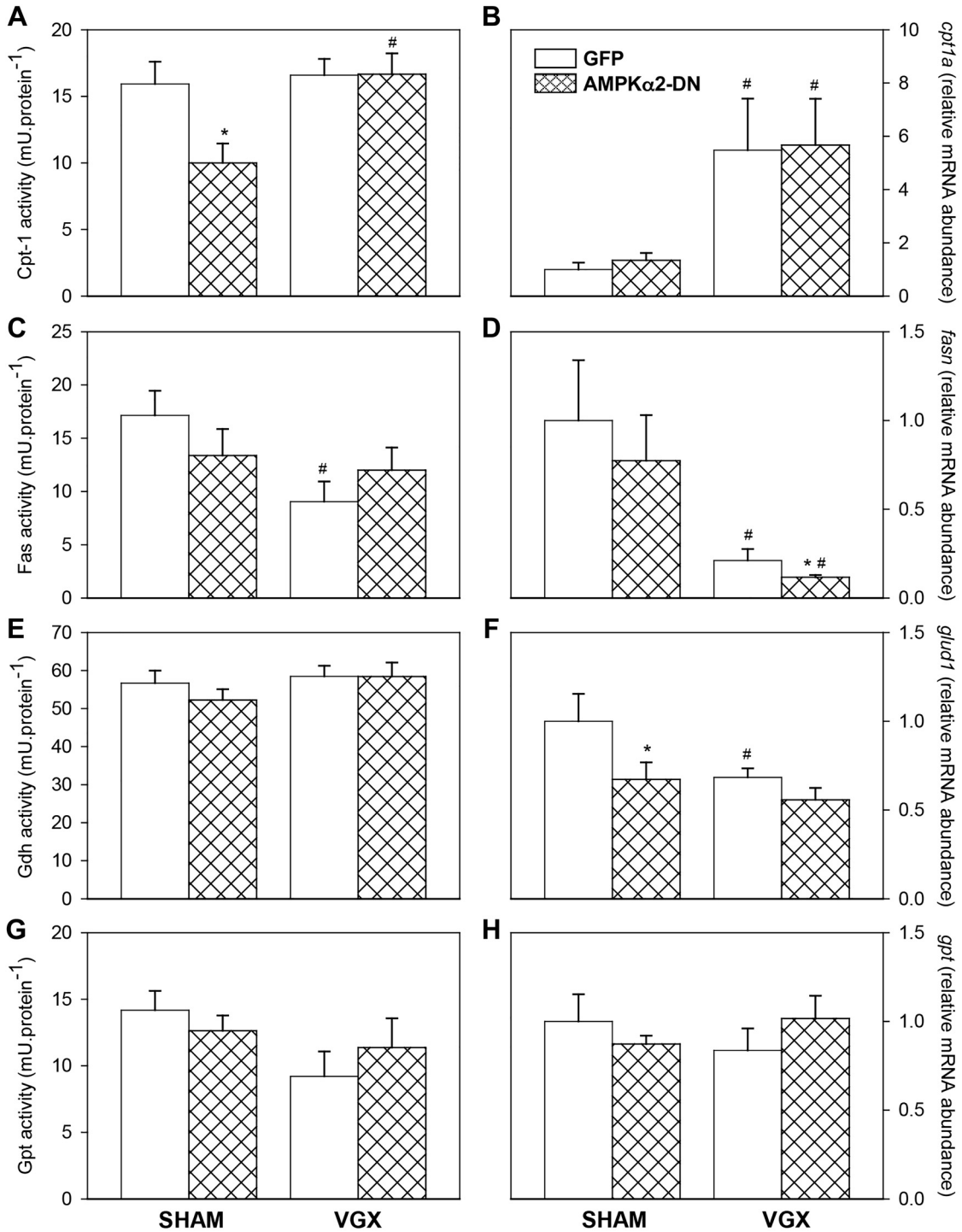


Fig. 7. Enzyme activity (*A*, *C*, *E*, and *G*) and mRNA abundance (*B*, *D*, *F*, and *H*) of carnitine palmitoyl transferase 1a [Cpt-1 (*cpt1a*)], fatty acid synthase [Fas (*fasn*)], glutamate dehydrogenase [Gdh (*glud1*)], and glutamate-pyruvate transaminase [Gpt (*gpt*)] in liver of rainbow trout 19 days after intracerebroventricular administration of adenovirus tagged with green fluorescent protein (GFP) or dominant negative isoform of AMPKα2 (AMPKα2-DN) in Sham or vagotomized (VGX) fish. Gene expression results are standardized to the control group and are normalized by β-actin (*actb*) and elongation factor 1α (*eef1a1*) expression. Each value is the mean ± SE of $n = 12$ (enzyme activities) or $n = 6$ (mRNA abundance) fish per group. *Significantly different ($P < 0.05$) from GFP within Sham or VGX; #significantly different ($P < 0.05$) from Sham within GFP or AMPKα2-DN.

eral, the central inhibition of AMPKα2 elicited reduced capacities for synthesis and use of glucose and lipids and reduced use of amino acids. The responses of glucose and lipid metabolism are comparable to those observed in mammals (40, 43, 60). Notably, as happens in mammals, some of these changes might relate to autonomic nervous system innervation of the liver since, in mammals, central inhibition of AMPK modulates the parasympathetic tone to the liver (12, 33). Therefore, we aimed to evaluate whether peripheral changes elicited by central inhibition of AMPKα2 disappeared in the absence of vagal

innervation to the liver. Before considering the impact of vagotomy on the effects of AMPKα2-DN treatment, we should consider the effects of vagotomy alone.

Several parameters were affected by vagotomy alone, as confirmed by changes observed when comparing VGX and Sham fish under GFP (control) treatment. Probably the most important change is the clear decrease observed in food intake in VGX fish, which is also found in mammals (14, 33) and was not related to the mRNA abundance of neuropeptides, which displayed no changes when comparing VGX and Sham fish after GFP treatment. Therefore, we may suggest that the effect of vagotomy on food intake might relate to the lack of information arriving to the brain from the periphery. In this way, it is important to remember that vagal afferent fibers have receptors for gastrointestinal hormones such as cholecystokinin (CCK), glucagon-like peptide 1 (GLP-1) or peptide YY (PYY) whose activation is known to affect food intake (6). Peripheral vagotomy also impacted metabolite levels in plasma, as demonstrated by increased levels of fatty acids and decreased levels of triglycerides. In the liver, changes attributable to vagotomy alone included decreased levels of glycogen, lactate, and fatty acids as well as decreased activities of Gck and Fas and mRNA abundance of *gck*, *fasn*, and *glud1* and increased activities of Fbpase and mRNA abundance of *cpt1a*. In general, changes elicited by vagotomy alone suggest a decreased use of glucose and amino acids as well as an increased use of lipids. It is interesting that in some cases (glucose and amino acids) the effects elicited by vagotomy are comparable to those elicited by AMPKα2-DN treatment alone. We have hypothesized that central inhibition of AMPKα2 is interpreted as a signal of satiety in the liver. Thus, it is reasonable that the lack of information arriving to the liver from the brain in VGX fish can be interpreted in the same way. This is the first study in fish reporting evidence of the metabolic effects of vagotomy since the few available studies focused on intestinal function (52).

A clear interaction between the effects of AMPKα2-DN treatment and vagotomy occurred in several parameters. Food intake displayed a similar trend when comparing the effect of AMPKα2-DN treatment in Sham or VGX fish though the difference in VGX fish was not significant ($P = 0.089$). This suggests that vagotomy, despite reducing food intake, does not further modulate the hypothalamic impact of AMPKα2 inhibition, which seems reasonable considering that food intake regulation occurs in the hypothalamus. In general, the effects observed in the periphery after AMPKα2-DN treatment in Sham fish disappeared when fish were vagotomized. These included, in plasma, changes in the levels of lactate, fatty acids, triglycerides, and amino acids. In liver, similar changes in response to AMPKα2-DN treatment in VGX fish occurred in the levels of glucose, glycogen, lactate, fatty acids, and amino acids as well as in the activities of Pfk, Fbpase, Cpt-1 and Fas and mRNA abundance of *gck*, *fasn*, *glud1*, and *gpt*. After AMPKα2 inhibition, no signals are sent to the liver, and therefore this tissue does not produce a metabolic response like that observed in Sham fish. As a whole, we suggest that several of the peripheral effects induced by central inhibition of AMPKα2 are blocked by vagotomy. The vagal flow is therefore required for the effects in liver of central inhibition of AMPKα2. No comparable studies have been performed in teleost fish, whereas in mammals, vagotomy was able to revert at least part of the metabolic changes induced in liver by central treatments affecting fatty acid sensing (19), leptin (10), sirtuin (18), activating transcription factor 4 (ATF-4; 62), orexin (13), NPY (20), thyroid hormones (34), and AMPKα1 modulation (10). However, we cannot exclude the involvement of additional mechanisms such as the hypothalamus-pituitary-interrenal axis since its mammalian equivalent (hypothalamus-pituitary-adrenal axis) is involved in the liver response to AMPK activation in the hypothalamus (17).

### *Perspectives and Significance*

We have demonstrated that the central inactivation of AMPKα2 resulting in food intake inhibition relates to changes in the mRNA abundance of hypothalamic neuropeptides. Furthermore, the changes observed in the liver in parameters related to glucose, amino acid, and lipid metabolism after central treatment with AMPKα2-DN mostly disappeared in vagotomized fish. These results support the idea that actions of hypothalamic AMPKα2 on liver metabolism are mediated by the autonomic nervous system thus providing new evidence regarding the involvement of central AMPKα2 in regulation of energy homeostasis in fish. Importantly, this evidence indicates that the well-established role of hypothalamic AMPK in energy balance is a canonical evolutionarily preserved mechanism that is also present in the fish lineage.

## ACKNOWLEDGMENTS

We thank Dr. Michael Axelsson (Department of Biological and Environmental Sciences, Faculty of Science, University of Gothenburg, Gothenburg, Sweden) for training M. Conde-Sieira in the vagotomy technique and for helpful comments.

## GRANTS

This study was supported by Spanish Agencia Estatal de Investigación and European Fund of Regional Development research grants to J. L. Soengas (AGL2016-74857-C3-1-R) and M. López (SAF2015-71026-R and RTI2018-101840-B-I00), Xunta de Galicia research grants (ED413B 2019/37 to J. L. Soengas and 2015-CP079 and 2016-PG068 to M. López), and an Atresmedia Corporation research grant (M. López). M. Conde-Sieira was the recipient of a Xunta de Galicia postdoctoral fellowship (ED481B2018/018). S. Comesaña was the recipient of a Spanish Ministerio de Educación, Cultura y Deporte predoctoral fellowship (Formación del Profesorado program; FPU16/00045).

## DISCLOSURES

No conflicts of interest, financial or otherwise, are declared by the authors.

## AUTHOR CONTRIBUTIONS

M.L. and J.L.S. conceived and designed research; M.C.-S., R.Á.-O., A.D.-R., C.V., and S.C. performed experiments; M.C.-S., V.C., R.Á.-O., A.D.-R., C.V., and S.C. analyzed data; M.C.-S., V.C., R.Á.-O., M.L., and J.L.S. interpreted results of experiments; M.C.-S., V.C., R.Á.-O., M.L., and J.L.S. prepared figures; M.C.-S., M.L., and J.L.S. drafted manuscript; M.L. and J.L.S. edited and revised manuscript; M.L. and J.L.S. approved final version of manuscript.

## REFERENCES

1. **Andersson U, Filipsson K, Abbott CR, Woods A, Smith K, Bloom SR, Carling D, Small CJ.** AMP-activated protein kinase plays a role in the control of food intake. *J Biol Chem* 279: 12005–12008, 2004. doi:10.1074/jbc.C300557200.
2. **Claret M, Smith MA, Batterham RL, Selman C, Choudhury AI, Fryer LG, Clements M, Al-Qassab H, Heffron H, Xu AW, Speakman JR, Barsh GS, Viollet B, Vaulont S, Ashford ML, Carling D, Withers DJ.** AMPK is essential for energy homeostasis regulation and glucose sensing by POMC and AgRP neurons. *J Clin Invest* 117: 2325–2336, 2007. doi:10.1172/JCI31516.

3. **Conde-Sieira M, Soengas JL.** Nutrient sensing systems in fish: impact on food intake regulation and energy homeostasis. *Front Neurosci* 10: 603, 2017. doi:10.3389/fnins.2016.00603.
4. **Conde-Sieira M, Capelli V, Álvarez-Otero R, Comesaña S, Liñares-Pose L, Velasco C, López M, Soengas JL.** Differential role of hypothalamic AMPKα isoforms in fish: an evolutive perspective. *Mol Neurobiol* 56: 5051–5066, 2019. doi:10.1007/s12035-018-1434-9.
5. **Contreras C, Nogueiras R, Diéguez C, Medina-Gómez G, López M.** Hypothalamus and thermogenesis: heating the BAT, browning the WAT. *Mol Cell Endocrinol* 438: 107–115, 2016. doi:10.1016/j.mce.2016.08.002.
6. **Cork SC.** The role of the vagus nerve in appetite control: Implications for the pathogenesis of obesity. *J Neuroendocrinol* 30: e12643, 2018. doi:10.1111/jne.12643.
7. **Craig PM, Moon TW.** Fasted zebrafish mimic genetic and physiological responses in mammals: a model for obesity and diabetes? *Zebrafish* 8: 109–117, 2011. doi:10.1089/zeb.2011.0702.
8. **Craig PM, Moyes CD, LeMoine CM.** Sensing and responding to energetic stress: evolution of the AMPK network. *Comp Biochem Physiol B Biochem Mol Biol* 224: 156–169, 2018. doi:10.1016/j.cbpb.2017.11.001.
9. **Delgado MJ, Cerdá-Reverter JM, Soengas JL.** Hypothalamic integration of metabolic, endocrine, and circadian signals in fish: involvement in the control of food intake. *Front Neurosci* 11: 354, 2017. doi:10.3389/fnins.2017.00354.
10. **German J, Kim F, Schwartz GJ, Havel PJ, Rhodes CJ, Schwartz MW, Morton GJ.** Hypothalamic leptin signaling regulates hepatic insulin sensitivity via a neurocircuit involving the vagus nerve. *Endocrinology* 150: 4502–4511, 2009. doi:10.1210/en.2009-0445.
11. **Gilmour KM, Craig PM, Dhillon RS, Lau GY, Richards JG.** Regulation of energy metabolism during social interactions in rainbow trout: a role for AMP-activated protein kinase. *Am J Physiol Regul Integr Comp Physiol* 313: R549–R559, 2017. doi:10.1152/ajpregu.00341.2016.
12. **Han SM, Namkoong C, Jang PG, Park IS, Hong SW, Katakami H, Chun S, Kim SW, Park JY, Lee KU, Kim MS.** Hypothalamic AMP-activated protein kinase mediates counter-regulatory responses to hypoglycaemia in rats. *Diabetologia* 48: 2170–2178, 2005. doi:10.1007/s00125-005-1913-1.
13. **Harada S, Yamazaki Y, Koda S, Tokuyama S.** Hepatic branch vagus nerve plays a critical role in the recovery of post-ischemic glucose intolerance and mediates a neuroprotective effect by hypothalamic orexin-A. *PLoS One* 9: e95433, 2014. doi:10.1371/journal.pone.0095433.
14. **Imbernon M, Beiroa D, Vázquez MJ, Morgan DA, Veyrat-Durebex C, Porteiro B, Díaz-Arteaga A, Senra A, Busquets S, Velásquez DA, Al-Massadi O, Varela L, Gándara M, López-Soriano FJ, Gallego R, Seoane LM, Argiles JM, López M, Davis RJ, Sabio G, Rohner-Jeanrenaud F, Rahmouni K, Dieguez C, Nogueiras R.** Central melanin-concentrating hormone influences liver and adipose metabolism via specific hypothalamic nuclei and efferent autonomic/JNK1 pathways. *Gastroenterology* 144: 636–649.e6, 2013. doi:10.1053/j.gastro.2012.10.051.
15. **Jorgensen SB, Rose AJ.** How is AMPK activity regulated in skeletal muscles during exercise? *Front Biosci* 13: 5589–5604, 2008. doi:10.2741/3102.
16. **Keppler D, Decker K.** Glycogen: determination with amyloglucosidase. In: *Methods of Enzymatic Analysis*, edited by Bergmeyer HU. New York: Academic, 1974, p. 1127–1131.
17. **Kinote A, Faria JA, Roman EA, Solon C, Razolli DS, Ignacio-Souza LM, Sollon CS, Nascimento LF, de Araújo TM, Barbosa AP, Lellis-Santos C, Velloso LA, Bordin S, Anhê GF.** Fructose-induced hypothalamic AMPK activation stimulates hepatic PEPCK and gluconeogenesis due to increased corticosterone levels. *Endocrinology* 153: 3633–3645, 2012. doi:10.1210/en.2012-1341.
18. **Knight CM, Gutierrez-Juarez R, Lam TK, Arrieta-Cruz I, Huang L, Schwartz G, Barzilai N, Rossetti L.** Mediobasal hypothalamic SIRT1 is essential for resveratrol's effects on insulin action in rats. *Diabetes* 60: 2691–2700, 2011. [Erratum in *Diabetes* 66: 3143–3144, 2017.] doi:10.2337/db10-0987.
19. **Lam TK, Pocai A, Gutierrez-Juarez R, Obici S, Bryan J, Aguilar-Bryan L, Schwartz GJ, Rossetti L.** Hypothalamic sensing of circulating fatty acids is required for glucose homeostasis. *Nat Med* 11: 320–327, 2005. doi:10.1038/nm1201.
20. **Li L, de La Serre CB, Zhang N, Yang L, Li H, Bi S.** Knockdown of neuropeptide Y in the dorsomedial hypothalamus promotes hepatic insulin sensitivity in male rats. *Endocrinology* 157: 4842–4852, 2016. doi:10.1210/en.2016-1662.
21. **Librán-Pérez M, Polakof S, López-Patiño MA, Míguez JM, Soengas JL.** Evidence of a metabolic fatty acid-sensing system in the hypothalamus and Brockmann bodies of rainbow trout: implications in food intake regulation. *Am J Physiol Regul Integr Comp Physiol* 302: R1340–R1350, 2012. doi:10.1152/ajpregu.00070.2012.
22. **Librán-Pérez M, Geurden I, Dias K, Corraze G, Panserat S, Soengas JL.** Feeding rainbow trout with a lipid-enriched diet: effects on fatty acid sensing, regulation of food intake and cellular signaling pathways. *J Exp Biol* 218: 2610–2619, 2015. doi:10.1242/jeb.123802.
23. **Lin SC, Hardie DG.** AMPK: sensing glucose as well as cellular energy status. *Cell Metab* 27: 299–313, 2018. doi:10.1016/j.cmet.2017.10.009.
24. **Lockie SH, Stark R, Mequinion M, Ch'ng S, Kong D, Spanswick DC, Lawrence AJ, Andrews ZB.** Glucose availability predicts the feeding response to ghrelin in male mice, an effect dependent on AMPK in AgRP neurons. *Endocrinology* 159: 3605–3614, 2018. doi:10.1210/en.2018-00536.
25. **López M.** EJE PRIZE 2017: Hypothalamic AMPK: a golden target against obesity? *Eur J Endocrinol* 176: R235–R246, 2017. doi:10.1530/EJE-16-0927.
26. **López M, Lage R, Saha AK, Pérez-Tilve D, Vázquez MJ, Varela L, Sangiao-Alvarellos S, Tovar S, Raghay K, Rodríguez-Cuenca S, Deoliveira RM, Castañeda T, Datta R, Dong JZ, Culler M, Sleeman MW, Álvarez CV, Gallego R, Lelliott CJ, Carling D, Tschöp MH, Diéguez C, Vidal-Puig A.** Hypothalamic fatty acid metabolism mediates the orexigenic action of ghrelin. *Cell Metab* 7: 389–399, 2008. doi:10.1016/j.cmet.2008.03.006.
27. **López M, Varela L, Vázquez MJ, Rodríguez-Cuenca S, González CR, Velagapudi VR, Morgan DA, Schoenmakers E, Agassandian K, Lage R, Martínez de Morentin PB, Tovar S, Nogueiras R, Carling D, Lelliott C, Gallego R, Oresic M, Chatterjee K, Saha AK, Rahmouni K, Diéguez C, Vidal-Puig A.** Hypothalamic AMPK and fatty acid metabolism mediate thyroid regulation of energy balance. *Nat Med* 16: 1001–1008, 2010. doi:10.1038/nm.2207.
28. **López M, Nogueiras R, Tena-Sempere M, Diéguez C.** Hypothalamic AMPK: a canonical regulator of whole-body energy balance. *Nat Rev Endocrinol* 12: 421–432, 2016. doi:10.1038/nrendo.2016.67.
29. **Magnoni LJ, Palstra AP, Planas JV.** Fueling the engine: induction of AMP-activated protein kinase in trout skeletal muscle by swimming. *J Exp Biol* 217: 1649–1652, 2014. doi:10.1242/jeb.099192.
30. **Martínez de Morentin PB, González CR, Saha AK, Martins L, Diéguez C, Vidal-Puig A, Tena-Sempere M, López M.** Hypothalamic AMP-activated protein kinase as a mediator of whole body energy balance. *Rev Endocr Metab Disord* 12: 127–140, 2011. doi:10.1007/s11154-011-9165-5.
31. **Martínez de Morentin PB, Whittle AJ, Fernø J, Nogueiras R, Diéguez C, Vidal-Puig A, López M.** Nicotine induces negative energy balance through hypothalamic AMP-activated protein kinase. *Diabetes* 61: 807–817, 2012. doi:10.2337/db11-1079.
32. **Martínez de Morentin PB, González-García I, Martins L, Lage R, Fernández-Mallo D, Martínez-Sánchez N, Ruíz-Pino F, Liu J, Morgan DA, Pinilla L, Gallego R, Saha AK, Kalsbeek A, Fliers E, Bisschop PH, Diéguez C, Nogueiras R, Rahmouni K, Tena-Sempere M, López M.** Estradiol regulates brown adipose tissue thermogenesis via hypothalamic AMPK. *Cell Metab* 20: 41–53, 2014. doi:10.1016/j.cmet.2014.03.031.
33. **Martínez-Sánchez N, Seoane-Collazo P, Contreras C, Varela L, Villarroya J, Rial-Pensado E, Buqué X, Aurrekoetxea I, Delgado TC, Vázquez-Martínez R, González-García I, Roa J, Whittle AJ, Gomez-Santos B, Velagapudi V, Tung YC, Morgan DA, Voshol PJ, Martínez de Morentin PB, López-González T, Liñares-Pose L, Gonzalez F, Chatterjee K, Sobrino T, Medina-Gómez G, Davis RJ, Casals N, Orešič M, Coll AP, Vidal-Puig A, Mittag J, Tena-Sempere M, Malagón MM, Diéguez C, Martínez-Chantar ML, Aspichueta P, Rahmouni K, Nogueiras R, Sabio G, Villarroya F, López M.** Hypothalamic AMPK-ER stress-JNK1 axis mediates the central actions of thyroid hormones on energy balance. *Cell Metab* 26: 212–229.e12, 2017. doi:10.1016/j.cmet.2017.06.014.
34. **Martínez-Sánchez N, Moreno-Navarrete JM, Contreras C, Rial-Pensado E, Fernø J, Nogueiras R, Diéguez C, Fernández-Real JM, López M.** Thyroid hormones induce browning of white fat. *J Endocrinol* 232: 351–362, 2017. doi:10.1530/JOE-16-0425.
35. **Martins L, Seoane-Collazo P, Contreras C, González-García I, Martínez-Sánchez N, González F, Zalvide J, Gallego R, Diéguez C, Nogueiras R, Tena-Sempere M, López M.** A functional link between

AMPK and orexin mediates the effect of BMP8B on energy balance. *Cell Rep* 16: 2231–2242, 2016. doi:10.1016/j.celrep.2016.07.045.

36. **McCrimmon RJ, Fan X, Cheng H, McNay E, Chan O, Shaw M, Ding Y, Zhu W, Sherwin RS.** Activation of AMP-activated protein kinase within the ventromedial hypothalamus amplifies counterregulatory hormone responses in rats with defective counterregulation. *Diabetes* 55: 1755–1760, 2006. doi:10.2337/db05-1359.
37. **Minokoshi Y, Alquier T, Furukawa N, Kim YB, Lee A, Xue B, Mu J, Foufelle F, Ferré P, Birnbaum MJ, Stuck BJ, Kahn BB.** AMP-kinase regulates food intake by responding to hormonal and nutrient signals in the hypothalamus. *Nature* 428: 569–574, 2004. doi:10.1038/nature02440.
38. **Moore S.** Amino acid analysis: aqueous dimethyl sulfoxide as solvent for the ninhydrin reaction. *J Biol Chem* 243: 6281–6283, 1968.
39. **Nilsson S.** Comparative anatomy of the autonomic nervous system. *Auton Neurosci* 165: 3–9, 2011. doi:10.1016/j.autneu.2010.03.018.
40. **Obici S, Feng Z, Morgan K, Stein D, Karkanias G, Rossetti L.** Central administration of oleic acid inhibits glucose production and food intake. *Diabetes* 51: 271–275, 2002. doi:10.2337/diabetes.51.2.271.
41. **O'Neill HM, Maarbjerg SJ, Crane JD, Jeppesen J, Jørgensen SB, Schertzer JD, Shyroka O, Kiens B, van Denderen BJ, Tarnopolsky MA, Kemp BE, Richter EA, Steinberg GR.** AMP-activated protein kinase (AMPK) β1β2 muscle null mice reveal an essential role for AMPK in maintaining mitochondrial content and glucose uptake during exercise. *Proc Natl Acad Sci USA* 108: 16092–16097, 2011. doi:10.1073/pnas.1105062108.
42. **Otero-Rodiño C, Velasco C, Álvarez-Otero R, López-Patiño MA, Míguez JM, Soengas JL.** Changes in the levels and phosphorylation status of Akt, AMPK, CREB and FoxO1 in hypothalamus of rainbow trout under conditions of enhanced glucosensing activity. *J Exp Biol* 220: 4410–4417, 2017. doi:10.1242/jeb.165159.
43. **Park S, Kim DS, Kang S, Shin BK.** Chronic activation of central AMPK attenuates glucose-stimulated insulin secretion and exacerbates hepatic insulin resistance in diabetic rats. *Brain Res Bull* 108: 18–26, 2014. doi:10.1016/j.brainresbull.2014.08.002.
44. **Pfaffl MW.** A new mathematical model for relative quantification in real-time RT-PCR. *Nucleic Acids Res* 29: e45, 2001. doi:10.1093/nar/29.9.e45.
45. **Polakof S, Soengas JL.** Involvement of lactate in glucose metabolism and glucosensing function in selected tissues of rainbow trout. *J Exp Biol* 211: 1075–1086, 2008. doi:10.1242/jeb.014050.
46. **Polakof S, Míguez JM, Moon TW, Soengas JL.** Evidence for the presence of a glucosensor in hypothalamus, hindbrain, and Brockmann bodies of rainbow trout. *Am J Physiol Regul Integr Comp Physiol* 292: R1657–R1666, 2007. doi:10.1152/ajpregu.00525.2006.
47. **Polakof S, Míguez JM, Soengas JL.** Dietary carbohydrates induce changes in glucosensing capacity and food intake of rainbow trout. *Am J Physiol Regul Integr Comp Physiol* 295: R478–R489, 2008. doi:10.1152/ajpregu.00176.2008.
48. **Polakof S, Álvarez R, Soengas JL.** Gut glucose metabolism in rainbow trout: implications in glucose homeostasis and glucosensing capacity. *Am J Physiol Regul Integr Comp Physiol* 299: R19–R32, 2010. doi:10.1152/ajpregu.00005.2010.
49. **Polakof S, Panserat S, Craig PM, Martyres DJ, Plagnes-Juan E, Savari S, Aris-Brosou S, Moon TW.** The metabolic consequences of hepatic AMP-kinase phosphorylation in rainbow trout. *PLoS One* 6: e20228, 2011. doi:10.1371/journal.pone.0020228.
50. **Rutter GA, da Silva Xavier G, Leclerc I.** Roles of 5′-AMP-activated protein kinase (AMPK) in mammalian glucose homoeostasis. *Biochem J* 375: 1–16, 2003. doi:10.1042/bj20030048.
51. **Seoane-Collazo P, Roa J, Rial-Pensado E, Liñares-Pose L, Beiroa D, Ruíz-Pino F, López-González T, Morgan DA, Pardavila JÁ, Sánchez-Tapia MJ, Martínez-Sánchez N, Contreras C, Fidalgo M, Diéguez C, Coppari R, Rahmouni K, Nogueiras R, Tena-Sempere M, López M.** SF1-specific AMPKα1 deletion protects against diet-induced obesity. *Diabetes* 67: 2213–2226, 2018. doi:10.2337/db17-1538.
52. **Seth H, Axelsson M.** Sympathetic, parasympathetic and enteric regulation of the gastrointestinal vasculature in rainbow trout (*Oncorhynchus mykiss*) under normal and postprandial conditions. *J Exp Biol* 213: 3118–3126, 2010. doi:10.1242/jeb.043612.
53. **Shi HJ, Xu C, Liu MY, Wang BK, Liu WB, Chen DH, Zhang L, Xu CY, Li XF.** Resveratrol improves the energy sensing and glycolipid metabolism of blunt snout bream *Megalobrama amblycephala* fed high-carbohydrate diets by activating the AMPK-SIRT1-PGC-1α network. *Front Physiol* 9: 1258, 2018. doi:10.3389/fphys.2018.01258.
54. **Soengas JL, Cerdá-Reverter JM, Delgado MJ.** Central regulation of food intake in fish: an evolutionary perspective. *J Mol Endocrinol* 60: R171–R199, 2018. doi:10.1530/JME-17-0320.
55. **Tanida M, Yamamoto N, Shibamoto T, Rahmouni K.** Involvement of hypothalamic AMP-activated protein kinase in leptin-induced sympathetic nerve activation. *PLoS One* 8: e56660, 2013. doi:10.1371/journal.pone.0056660.
56. **Velasco C, Otero-Rodiño C, Comesaña S, Míguez JM, Soengas JL.** Hypothalamic mechanisms linking fatty acid sensing and food intake regulation in rainbow trout. *J Mol Endocrinol* 59: 377–390, 2017. doi:10.1530/JME-17-0148.
57. **Viollet B, Andreelli F, Jørgensen SB, Perrin C, Flamez D, Mu J, Wojtaszewski JF, Schuit FC, Birnbaum M, Richter E, Burcelin R, Vaulont S.** Physiological role of AMP-activated protein kinase (AMPK): insights from knockout mouse models. *Biochem Soc Trans* 31: 216–219, 2003. doi:10.1042/bst0310216.
58. **Whittle AJ, Carobbio S, Martins L, Slawik M, Hondares E, Vázquez MJ, Morgan D, Csikasz RI, Gallego R, Rodriguez-Cuenca S, Dale M, Virtue S, Villarroya F, Cannon B, Rahmouni K, López M, Vidal-Puig A.** BMP8B increases brown adipose tissue thermogenesis through both central and peripheral actions. *Cell* 149: 871–885, 2012. doi:10.1016/j.cell.2012.02.066.
59. **Xu C, Liu WB, Zhang DD, Cao XF, Shi HJ, Li XF.** Interactions between dietary carbohydrate and metformin: implications on energy sensing, insulin signaling pathway, glycolipid metabolism and glucose tolerance in blunt snout bream *Megalobrama amblycephala*. *Aquaculture* 483: 183–195, 2018. doi:10.1016/j.aquaculture.2017.10.022.
60. **Yang CS, Lam CK, Chari M, Cheung GW, Kokorovic A, Gao S, Leclerc I, Rutter GA, Lam TK.** Hypothalamic AMP-activated protein kinase regulates glucose production. *Diabetes* 59: 2435–2443, 2010. doi:10.2337/db10-0221.
61. **Zeng L, Liu B, Wu CW, Lei JL, Xu MY, Zhu AY, Zhang JS, Hong WS.** Molecular characterization and expression analysis of AMPK α subunit isoform genes from *Scophthalmus maximus* responding to salinity stress. *Fish Physiol Biochem* 42: 1595–1607, 2016. doi:10.1007/s10695-016-0243-1.
62. **Zhang Q, Yu J, Liu B, Lv Z, Xia T, Xiao F, Chen S, Guo F.** Central activating transcription factor 4 (ATF4) regulates hepatic insulin resistance in mice via S6K1 signaling and the vagus nerve. *Diabetes* 62: 2230–2239, 2013. doi:10.2337/db12-1050.